Nonlinear Dyn (2021) 104:4045–4061
https://doi.org/10.1007/s11071-021-06454-8

ORIGINAL PAPER

Parameter identification of nonlinear systems with time-delay from time-domain data

Tao Zhang · Zhong-rong Lu · Ji-ke Liu · Guang Liu

Received: 25 November 2020 / Accepted: 9 April 2021 / Published online: 23 April 2021

Abstract The present paper develops an enhanced response sensitivity approach for parameter identification of nonlinear time-delay systems from the time-domain data. Accurate and rapid identification of the time-delay system's parameters is the key to achieve effective control and synchronization, especially for the delay parameters. The work of this paper is mainly threefold. Firstly, taking a general nonlinear time-delay system as the investigated object, the characteristics of the nonlinear time-delay system are introduced, and the response sensitivity analysis with respect to the system parameters is derived. Then, the problem of parameter identification is modeled as a nonlinear least-squares optimization function. To this end, a novel iteration-based approach is developed to solve such problem, and the ill-posed situation is tackled by Tikhonov regularization. Besides, the trust-region constraint is implemented to enhance the convergence of the algorithm. Finally, the feasibility of the proposed approach is verified by two numerical examples and a real electronic circuit experiment. The results proved that the proposed approach can identify parameters of nonlinear time-delay systems accurately, robustly and effectively.

Keywords Parameter identification · Nonlinear time-delay system · Trust-region constraint · Enhanced response sensitivity approach · Time-domain data

T. Zhang · Z. Lu · J. Liu · G. Liu (✉)
School of Aeronautics and Astronautics, Sun Yat-sen University, Guangzhou, People's Republic of China
e-mail: owenyaa@163.com

1 Introduction

Time-delay phenomenon often appears in engineering systems, such as mechanics [1], circuits [2], optics [3], biology [4], medicine [5], and so on [6–9]. In these systems, due to the existence of time-delay, the mechanical behavior of the system is determined not only by the current state, but also by the system's state in the past time. The introduction of time-delay usually leads to destabilization and more complex dynamic behavior. At the same time, the parameters related to time-delay are unknown in most systems. In addition, in order to realize the control and synchronization of nonlinear time-delay systems, we usually need to know the exact values of the system's parameters (especially the delay parameter) rather than the design values [10]. Therefore, identifying the parameters of nonlinear time-delay systems accurately and quickly is an essential preparatory step for applying these systems. However, due to some inherent characteristics of nonlinear time-delay systems, it is still a demanding task to identify their parameters.

Generally, the identification of nonlinear time-delay system parameters from measured response data belongs to an inverse problem. The inverse problem is formulated as an optimization problem whose objective function is commonly defined as the weighted least-squares of the error between the measured response data and calculated response data [11]. Methods for such optimization problems can be broadly divided into

two categories: meta-heuristic algorithms and gradient-based methods. The meta-heuristic algorithms such as genetic algorithm [12] , artificial bee colony algorithm [13] , particle swarm optimization algorithm [14] and chaotic ant swarm algorithm [15] have been widely used in parameter identification of time-delay systems. Such meta-heuristic algorithms have the advantage that strong capability in global searching and good robustness, and they do not require the system to have strict continuity and differentiability. However, due to its random search characteristics, meta-heuristics algorithms usually have redundant iterations, and the calculation process is very time-consuming, and even different results may be obtained by each calculation.

In contrast, the gradient-based methods such as Newton's method [16] and sensitivity method [17] usually have faster convergence rate. Among these gradient-based methods, the sensitivity-based method in either frequency or time domain is the most commonly used. However, due to the complexity of sensitivity analysis, it is challenging work to identify the parameters of nonlinear time-delay systems by the sensitivity-based methods. Recently, a response sensitive framework based on time-domain data was proposed by Lu et al. [18], and it has been extended to parameter estimation of many systems by Lu and his collaborators. Furthermore, Lu et al. [19] enhanced the response sensitivity method by introducing the trust region constraint, and used this method to detect the damage of building structures. Moreover, this method has already been proved to be weakly convergent. Subsequently, the enhanced response sensitivity approach (ERSA) has been successfully applied to the parameter identification of chaotic systems [20], fractional-order systems [21,22].

In addition to the time-domain method, the frequency-domain method based on the frequency response function can also identify the parameters of time-delay systems [23,24]. Liu et al. [25] proposed a fast parameter identification approach for time-delay system from frequency-domain data. Although this rapid frequency-domain approach is effective, it is only applicable for linear time-delay systems. For nonlinear time-delay system, Zhang and Xu [26] investigated a harmonic balance-based method to identify parameters by using noise-free measurement data. To further deal with the distortion in the output measurement data, Zhang et al. [27] proposed an identification algorithm based on the harmonic coefficient increment of periodic response, and the parameters were identified and the distortion calculation was corrected. With that, Zhang et al. [28] developed a complete architecture of the adaptive-noise-correction integrated parameter identification method from the periodic responses.

Moreover, compared with the frequency-domain method, only a small amount of frequency-domain data can be obtained even if a lot of sensors are arranged. The time-domain data are usually easier to obtain in practical engineering, and even only one sensor can obtain enough time-domain data. In this paper, a unified framework is proposed to identify the parameters of nonlinear time-delay systems through sensitivity analysis. The measurement data type of this method can be arbitrary single or combined time-domain data, which not only has weak convergence, but also can be applied to general linear or nonlinear time-delay systems.

The rest of the paper is organized as follows: In Sect. 2, a general model of the nonlinear time-delay system is established, and the sensitivity analysis with respect to the corresponding parameters is derived. In Sect. 3, the ERSA and specific procedures are introduced. The performance of the proposed approach is evaluated in Sect. 4 by two numerical examples: a van der Pol-Duffing system with multiple time-delay feedback, a multi-degree-of-freedom energy harvesting (EH) time-delay system, respectively. In Sect. 5, a Mackey-Glass experimental test is investigated in to verify the performance of the proposed approach, and the conclusions are drawn in Sect. 6.

2 Problem statement

First of all, some characteristics of nonlinear time-delay systems are listed as follows:

- Because the system contains both nonlinearity and delay, even the delay systems with low degrees-of-freedom (DOF) will exhibit complex dynamic behaviors such as periodic, aperiodic or chaotic responses.
- Nonlinear time-delay systems can be described by a delay differential equation (DDE): $\dot{x} = f(x(t), x(t-\tau))$, which has some properties that ordinary differential equations do not have. Due to the delay effect, the behavior of the system after $t > t_0$ is related not only to the current state $x(t_0)$ but also to the state in $[t_0 - \tau, t_0]$.

– The characteristic equation of the time-delay system is a transcendental equation, which has infinite eigenvalues, and the solution space is also infinite dimension.
– The slight delay effect of the system can be sometimes ignored in actual project. With $\tau = 0$, the nonlinear time-delay equation degenerates into an ordinary differential equation. However, some special phenomena can only be reasonably explained when the delay effect is considered.

A general form of nonlinear time delay system with n-DOF is considered:

$$\begin{cases} \mathscr{L}(\ddot{\boldsymbol{x}}, \dot{\boldsymbol{x}}, \boldsymbol{x}, t, \mathbb{T}) + \mathscr{N}(\ddot{\boldsymbol{x}}, \dot{\boldsymbol{x}}, \boldsymbol{x}, t, \mathbb{T}') = \mathscr{F}(t, \mathbb{T}''), \quad t > 0 \\ \boldsymbol{x}(t) = \boldsymbol{x_0}, \dot{\boldsymbol{x}}(t) = \dot{\boldsymbol{x}}_{\boldsymbol{0}}, \quad t \le 0 \end{cases} \tag{1}$$

where $\mathscr{L}$, $\mathscr{N}$ and $\mathscr{F}$ are the linear, nonlinear and external excitation part of the system, respectively. The linear operator $\mathscr{L}$ and the nonlinear operator $\mathscr{N}$ may contain the displacement x, velocity $\dot{x}$ or acceleration $\ddot{x}$, and may also contain the delay term. $\boldsymbol{x} = [x_1, x_2, \ldots, x_n]^{\mathrm{T}}$ is the displacement vector, $\dot{\boldsymbol{x}}$ and $\ddot{\boldsymbol{x}}$ correspond to the velocity and acceleration vectors, where the dots over the variable represents the differential with respect to the time t. And $\boldsymbol{x}_0$ and $\dot{\boldsymbol{x}}_0$ are the initial displacement and velocity conditions of the system. $\mathbb{T}$, $\mathbb{T}'$ and $\mathbb{T}''$ are defined as delay parameter vectors of linear part, nonlinear part and external excitation part, respectively, and they have the following form:

$$\begin{cases} \mathbb{T} = [\tau_1, \tau_2, \ldots, \tau_l]^{\mathrm{T}} \\ \mathbb{T}' = [\tau_1', \tau_2', \ldots, \tau_m']^{\mathrm{T}} \\ \mathbb{T}'' = [\tau_1'', \tau_2'', \ldots, \tau_n'']^{\mathrm{T}} \end{cases} \tag{2}$$

For delay differential systems, even linear systems are difficult to obtain their analytical solutions. The response of the time-delay system is usually obtained by numerical methods, such as linear multistep method, Runge–Kutta (RK) method, collocation method [29], and so on. The numerical responses of this paper are obtained by solving delay differential systems by "dde23" function in MATLAB.

2.1 The sensitivity analysis in time-domain

The unknown parameter of nonlinear time-delay system is marked as $\boldsymbol{a} = [a_1, a_2, \ldots, a_p]$, which can be any system parameter in linear operator $\mathscr{L}$, the nonlinear operator $\mathscr{N}$ and external excitation $\mathscr{F}$, or delay parameter in $\mathbb{T}$, $\mathbb{T}'$ and $\mathbb{T}''$. The response sensitivity to the unknown parameters of the nonlinear time-delay system can be obtained as follows:

$$a_i \in \boldsymbol{a} \ldots \frac{\partial \boldsymbol{x}}{\partial a_i}, \frac{\partial \dot{\boldsymbol{x}}}{\partial a_i}, \frac{\partial \ddot{\boldsymbol{x}}}{\partial a_i}, \quad i = 1, 2, \ldots, p \tag{3}$$

It should be noted that the response $\boldsymbol{x}(t)$ is an implicit function with respect to the unknown parameters, i.e., $\boldsymbol{x}(\boldsymbol{a}, t)$. The similar situation is also applicable to the time-delay term $\boldsymbol{x}(t - \tau_j) = \boldsymbol{x}(\boldsymbol{a}, t - \tau_j), (\tau_j \in \{\mathbb{T}, \mathbb{T}', \mathbb{T}''\})$.

For the response sensitivity analysis with respect to the unknown parameters $a_i \in \hat{\boldsymbol{a}}$ (except the delay parameters τ), taking the differential on both sides of the equation (1),

$$\begin{cases} \mathscr{L}\left(\frac{\partial \ddot{\boldsymbol{x}}}{\partial a_i}, \frac{\partial \dot{\boldsymbol{x}}}{\partial a_i}, \frac{\partial \boldsymbol{x}}{\partial a_i}, t, \mathbb{T}\right) + \mathscr{N}\left(\frac{\partial \ddot{\boldsymbol{x}}}{\partial a_i}, \frac{\partial \dot{\boldsymbol{x}}}{\partial a_i}, \frac{\partial \boldsymbol{x}}{\partial a_i}, t, \mathbb{T}'\right) \\ \quad = \frac{\partial \mathscr{F}(t, \mathbb{T}'')}{\partial a_i} - \frac{\partial \mathscr{L}(\ddot{\boldsymbol{x}}, \dot{\boldsymbol{x}}, \boldsymbol{x}, t, \mathbb{T})}{\partial a_i} \\ \qquad - \frac{\partial \mathscr{N}(\ddot{\boldsymbol{x}}, \dot{\boldsymbol{x}}, \boldsymbol{x}, t, \mathbb{T}')}{\partial a_i} \\ \frac{\partial \boldsymbol{x_0}}{\partial a_i} = \boldsymbol{0}, \frac{\partial \dot{\boldsymbol{x}}_{\boldsymbol{0}}}{\partial a_i} = \boldsymbol{0} \end{cases} \tag{4}$$

The response sensitivity analysis of time-delay parameters $\tau_j \in \{\mathbb{T}, \mathbb{T}', \mathbb{T}''\}$ is in the another form, for example, as for $\tau_j \in \mathbb{T}$, assuming the time-delay parameter appears in displacement vector, i.e., $x(t - \tau_j)$, there is

$$\begin{aligned} &\frac{\mathrm{d}\boldsymbol{x}(t - \tau_j)}{\mathrm{d}\tau_j} = \frac{\partial \boldsymbol{x}(t - \tau_j)}{\partial \tau_j} - \boldsymbol{D}_j \dot{\boldsymbol{x}}(t - \tau_j); \\ &\boldsymbol{D}_j = \mathrm{diag}\left(\frac{\partial \mathbb{T}}{\partial \tau_j}\right) \end{aligned} \tag{5}$$

where $\boldsymbol{D}_j$ is a diagonal matrix with diagonal elements given by $\frac{\partial \mathbb{T}}{\partial \tau_j}$. So the sensitivity equation with respect to $\tau_j \in \mathbb{T}$ can be obtained as follows:

$$\begin{cases} \mathscr{L}\left(\frac{\partial \ddot{\boldsymbol{x}}}{\partial \tau_j}, \frac{\partial \dot{\boldsymbol{x}}}{\partial \tau_j}, \frac{\partial \boldsymbol{x}(t - \tau_j)}{\partial \tau_j}, t\right) + \mathscr{N}\left(\frac{\partial \ddot{\boldsymbol{x}}}{\partial \tau_j}, \frac{\partial \dot{\boldsymbol{x}}}{\partial \tau_j}, \frac{\partial \boldsymbol{x}}{\partial \tau_j}, t, \mathbb{T}'\right) \\ \quad = \frac{\partial \mathscr{F}(t, \mathbb{T}'')}{\partial \tau_j} + \mathscr{L}(\ddot{\boldsymbol{x}}, \dot{\boldsymbol{x}}, \boldsymbol{D}_j \dot{\boldsymbol{x}}(t - \tau_j), t), \\ \quad \boldsymbol{D}_j = \mathrm{diag}\left(\frac{\partial \mathbb{T}}{\partial \tau_j}\right) \\ \frac{\partial \boldsymbol{x_0}}{\partial \tau_j} = \boldsymbol{0}, \frac{\partial \dot{\boldsymbol{x}}_{\boldsymbol{0}}}{\partial \tau_j} = \boldsymbol{0} \end{cases} \tag{6}$$

Of course, the time-delay parameters can also appear in the nonlinear part $\mathscr{N}$ or external excitation $\mathscr{F}$, and the system may also contain the velocity delay $\dot{x}(t - \tau_j)$ or acceleration delay $\ddot{x}(t - \tau_j)$. The relevant sensitivity equations are also obtained in the above way. Moreover, Eqs. (6) and (4) belong to similar delay differential equations, so Eq. (6) can also be solved by 'dde23' function.

3 Identifying the unknown parameters from the time-domain data

Next, we propose a unified framework to identify/recover parameters of the time-delay system from the measured time-domain data. In real engineering, the time-domain data obtained by various sensors can be the displacement, velocity or acceleration data of the system, which are usually distributed on a series of time nodes $0 = t_0 < t_1 < t_2 < \cdots < t_m = T$, as follows:

$$\hat{\boldsymbol{R}} = \begin{pmatrix} [\hat{x}_j(t_1), \hat{x}_j(t_2), \ldots, \hat{x}_j(t_m)]^{\mathrm{T}} \\ [\hat{\dot{x}}_k(t_1), \hat{\dot{x}}_k(t_2), \ldots, \hat{\dot{x}}_k(t_m)]^{\mathrm{T}} \\ [\hat{\ddot{x}}_l(t_1), \hat{\ddot{x}}_l(t_2), \ldots, \hat{\ddot{x}}_l(t_m)]^{\mathrm{T}} \end{pmatrix} \tag{7}$$

where the hat over symbol indicates that the variable is measurement data, $\hat{x}_j$ represents the measured displacement of the j-th DOF, and $\hat{\dot{x}}_k$ and $\hat{\ddot{x}}_l$ correspond to the measured velocity data of the k-th DOF and the acceleration data of the l-th DOF, respectively. Correspondingly, the numerical response of Eq. (1) obtained by numerical method can be expressed as:

$$\boldsymbol{R}(\boldsymbol{a}) = \begin{pmatrix} [x_j(t_1, \boldsymbol{a}), x_j(t_2, \boldsymbol{a}), \ldots, x_j(t_m, \boldsymbol{a})]^{\mathrm{T}} \\ [\dot{x}_k(t_1, \boldsymbol{a}), \dot{x}_k(t_2, \boldsymbol{a}), \ldots, \dot{x}_k(t_m, \boldsymbol{a})]^{\mathrm{T}} \\ [\ddot{x}_l(t_1, \boldsymbol{a}), \ddot{x}_l(t_2, \boldsymbol{a}), \ldots, \ddot{x}_l(t_m, \boldsymbol{a})]^{\mathrm{T}} \end{pmatrix} \tag{8}$$

Obviously, the calculated response $\boldsymbol{R}(\boldsymbol{a})$ is an implicit function of time t and unknown parameters $\boldsymbol{a}$. Up to now, identifying/recovering the unknown parameters $\boldsymbol{a} = [a_1, a_2, \ldots, a_p]$ of the time-delay system from the measured data can be expressed as: for system (1), find a set of parameters $\boldsymbol{a}$ so that the residual error between the calculated numerical response $\boldsymbol{R}(\boldsymbol{a})$ and the measured time-domain data $\hat{\boldsymbol{R}}$ is the minimum. Such a parameter identification/estimation problem can be formulated as a nonlinear minimum least-squares optimization problem,

$$\boldsymbol{a}^* = \arg\min_{\boldsymbol{a} \in \mathbb{A}} \left\{ \mathscr{G}(\boldsymbol{a}) := \|\hat{\boldsymbol{R}} - \boldsymbol{R}(\boldsymbol{a})\|_{\mathbf{W}}^2 \right\} \tag{9}$$

where $\mathscr{G}(\boldsymbol{a})$ is the nonlinear minimum least-squares objective function, and all parameters $\boldsymbol{a}$ are optimized in the feasible region $\mathbb{A}$. $\|(\cdot)\|_{\mathbf{W}} = \sqrt{(\cdot)^{\mathrm{T}}\mathbf{W}(\cdot)}$ represents the ℓ^2-norm of a positive defined weighting matrix $\mathbf{W}$. The weight matrix $\mathbf{W}$ plays an important role in problem (9). A good weight matrix can improve the accuracy of identification, and may accelerate the convergence process. Lu et al. [30] have proved that the reciprocal of the covariance of measurement data error is the optimal weight matrix. This paper will also discuss the influence of the weight matrix on the parameter identification of the time-delay system. When the weight matrix is selected as the identity matrix ($\boldsymbol{I}$), it means that the weight matrix is not considered.

For the nonlinear optimization problem like Eq. (9), it can be solved by iterative method, that is, given an initial value $\boldsymbol{a}^{(0)}$, it can be iterated in the following form:

$$\boldsymbol{a}^{(k)} = \boldsymbol{a}^{(k-1)} + \delta\boldsymbol{a}^{(k)}, k = 1, 2, 3 \ldots \tag{10}$$

until the nonlinear objective function $\mathscr{G}(\boldsymbol{a})$ converges. $\delta\boldsymbol{a}$ is the iterative updating quantity. Therefore, the key to the problem (9) is how to quickly determine a reasonable iteration update $\delta\boldsymbol{a}$ according to the current parameter $\bar{\boldsymbol{a}}$ in each iteration. A feasible way is to linearize the nonlinear objective function $\mathscr{G}(\bar{\boldsymbol{a}} + \delta\boldsymbol{a})$ near the current parameter $\bar{\boldsymbol{a}}$ to obtain the approximate linear objective function $\hat{\mathscr{G}}(\delta\boldsymbol{a}, \bar{\boldsymbol{a}})$, so that the original nonlinear optimization problem is approximated as a linear problem as follows:

$$\hat{\mathscr{G}}(\delta\boldsymbol{a}, \bar{\boldsymbol{a}}) = ||\delta\boldsymbol{R}(\bar{\boldsymbol{a}}) - \boldsymbol{S}(\bar{\boldsymbol{a}})\delta\boldsymbol{a}||_{\mathbf{W}}^2 \tag{11}$$

where $\delta\boldsymbol{R}(\bar{\boldsymbol{a}}) := \hat{\boldsymbol{R}} - \boldsymbol{R}(\bar{\boldsymbol{a}})$, $\boldsymbol{S}$ is the first-order response sensitivity matrix of the response $\boldsymbol{R}(\bar{\boldsymbol{a}})$, and it is in the form of

$$\begin{aligned} \boldsymbol{S}(\bar{\boldsymbol{a}}) = \nabla_a \boldsymbol{R}(\bar{\boldsymbol{a}}) = \nabla_a \begin{pmatrix} x_j(t_1) \\ \vdots \\ x_j(t_m) \\ \dot{x}_k(t_1) \\ \vdots \\ \dot{x}_k(t_m) \\ \ddot{x}_l(t_1) \\ \vdots \\ \ddot{x}_l(t_m) \end{pmatrix} \\ = \begin{pmatrix} \frac{\partial x_j(t_1)}{\partial a_1}, \frac{\partial x_j(t_1)}{\partial a_2} \cdots \frac{\partial x_j(t_1)}{\partial a_p} \\ \vdots \\ \frac{\partial x_j(t_m)}{\partial a_1}, \frac{\partial x_j(t_m)}{\partial a_2} \cdots \frac{\partial x_j(t_m)}{\partial a_p} \\ \frac{\partial \dot{x}_k(t_1)}{\partial a_1}, \frac{\partial \dot{x}_k(t_1)}{\partial a_2} \cdots \frac{\partial \dot{x}_k(t_1)}{\partial a_p} \\ \vdots \\ \frac{\partial \dot{x}_k(t_m)}{\partial a_1}, \frac{\partial \dot{x}_k(t_m)}{\partial a_2} \cdots \frac{\partial \dot{x}_k(t_m)}{\partial a_p} \\ \frac{\partial \ddot{x}_l(t_1)}{\partial a_1}, \frac{\partial \ddot{x}_l(t_1)}{\partial a_2} \cdots \frac{\partial \ddot{x}_l(t_1)}{\partial a_p} \\ \vdots \\ \frac{\partial \ddot{x}_l(t_m)}{\partial a_1}, \frac{\partial \ddot{x}_l(t_m)}{\partial a_2} \cdots \frac{\partial \ddot{x}_l(t_m)}{\partial a_p} \end{pmatrix} \end{aligned} \tag{12}$$

where $\frac{\partial x_j(t_q)}{\partial a_i}, \frac{\partial \dot{x}_k(t_q)}{\partial a_i}$ and $\frac{\partial \ddot{x}_l(t_q)}{\partial a_i}$ $(q = 1, 2, \ldots, m; i = 1, 2, \ldots, p)$ are the displacement sensitivity, velocity sensitivity and acceleration sensitivity, respectively,

and can be obtained according to Eqs. (4), (5). However, there is still a problem with the above approximate objective function $\hat{\mathscr{G}}(\delta\boldsymbol{a}, \bar{\boldsymbol{a}})$, such as ill-posed in the iterative process. In this case, the Tikhonov regularization can be further introduced to deal with such ill-posed situation, and Eq. (12) is further transformed into

$$\begin{aligned}\delta\boldsymbol{a}_\lambda &= \arg\min_{\delta\boldsymbol{a}} ||\delta\boldsymbol{R}(\bar{\boldsymbol{a}}) - \boldsymbol{S}(\bar{\boldsymbol{a}})\delta\boldsymbol{a}||_{\mathbf{W}}^2 + \lambda||\delta\boldsymbol{a}||^2 \\ &= \left[S^{\mathrm{T}}(\bar{\boldsymbol{a}})\mathbf{W}S(\bar{\boldsymbol{a}}) + \lambda\mathbf{I}\right]^{-1} S^{\mathrm{T}}(\bar{\boldsymbol{a}})\mathbf{W}\delta\boldsymbol{R}(\bar{\boldsymbol{a}})\end{aligned} \tag{13}$$

where $\lambda \geq 0$ is named as the regularization parameter, $\mathbf{I}$ is the identity matrix. Different regularization parameter will lead to different update $\delta\boldsymbol{a}$, and there is a common way to determine the appropriate regularization parameter is the L-curve method [31,32]. The essence of Tikhonov regularization is to balance the proportion between the fitting residual $\|\delta R\,(\bar{\boldsymbol{a}}) - S\,(\bar{\boldsymbol{a}})\,\delta\boldsymbol{a}\|^2$ and the update $\|\delta\boldsymbol{a}\|^2$. The regularization parameter λ determined by the L-curve method is registered as $\lambda_L(\bar{\boldsymbol{a}})$.

Even so, the L-curve method only aims at approximate linear objective function $\hat{\mathscr{G}}(\delta\boldsymbol{a}, \bar{\boldsymbol{a}})$ instead of original nonlinear objective function $\mathscr{G}(\bar{\boldsymbol{a}})$, which makes this method only suitable for weak nonlinear problems. In order to determine more reasonable λ and $\delta\boldsymbol{a}$ for the strongly nonlinear time-delay systems, the *trust-region constraint* is introduced. The iterative updating quantity $\delta\boldsymbol{a}$ should be small enough to ensure $\hat{\mathscr{G}}(\delta\boldsymbol{a}, \bar{\boldsymbol{a}})$ agrees well with $\mathscr{G}(\bar{\boldsymbol{a}}+\delta\boldsymbol{a})$. The approximate degree of $\hat{\mathscr{G}}(\delta\boldsymbol{a}, \bar{\boldsymbol{a}})$ and $\mathscr{G}(\bar{\boldsymbol{a}})$ can be measured by the following *agreement indicator*

$$\begin{aligned}\vartheta(\delta\boldsymbol{a}, \bar{\boldsymbol{a}}) &= \frac{\mathscr{G}(\bar{\boldsymbol{a}}) - \mathscr{G}(\bar{\boldsymbol{a}} + \delta\boldsymbol{a})}{\hat{\mathscr{G}}(0, \bar{\boldsymbol{a}}) - \hat{\mathscr{G}}(\delta\boldsymbol{a}, \bar{\boldsymbol{a}})} \\ &= \frac{\|\delta\boldsymbol{R}(\bar{\boldsymbol{a}})\|_{\boldsymbol{W}}^2 - \|\delta\boldsymbol{R}(\bar{\boldsymbol{a}} + \delta\boldsymbol{a})\|_{\boldsymbol{W}}^2}{\|\delta\boldsymbol{R}(\bar{\boldsymbol{a}})\|_{\boldsymbol{W}}^2 - \|\delta\boldsymbol{R}(\bar{\boldsymbol{a}}) - \boldsymbol{S}(\bar{\boldsymbol{a}})\delta\boldsymbol{a}\|_{\boldsymbol{W}}^2}\end{aligned} \tag{14}$$

When the *agreement indicator* satisfies the following conditions in each iteration,

$$\vartheta(\delta\boldsymbol{a}, \bar{\boldsymbol{a}}) \geq \vartheta_{cr} \in [0.25, 0.75] \tag{15}$$

The *trust-region constraint* enhances that the linearized objective function is close enough to the original nonlinear objective function. Furthermore, with $\|S^{\mathrm{T}}(\bar{\boldsymbol{a}})\mathbf{W}\delta R(\bar{\boldsymbol{a}})\|^2 \neq 0$, there are

$$\begin{cases} \lim\limits_{\lambda\to+\infty} \vartheta(\delta\boldsymbol{a}, \bar{\boldsymbol{a}}) = 1 > \vartheta_{cr} \\ \lim\limits_{\lambda\to+\infty} \|\delta\boldsymbol{a}_\lambda\| = 0 \end{cases} \tag{16}$$

Equation (16) means that with regularization parameter λ large enough, the update $||\delta\boldsymbol{a}_\lambda||$ will be small enough and the *trust-region constraint* (15) will always be satisfied, that is, the approximate linear objective function will become back into the original nonlinear objective function again. This indicates that there is a critical regularization parameter λ_{cr} such that the *agreement condition* is satisfied as long as $\lambda \geq \lambda_{cr}$. Above all, the response sensitivity approach with the *trust-region constraint* can be named as the enhanced response sensitivity approach (ERSA). Moreover, the algorithm is proved to have weak convergence [19]

$$\lim_{k\to 0} ||\nabla_{\boldsymbol{a}}\mathscr{G}(\boldsymbol{a}^{(k)}, t)|| = 0 \tag{17}$$

Finally, the algorithm procedure of the parameter identification of ERSA is outlined in Table 1.

4 Numerical examples

In this section, two numerical examples concerning a van der Pol-Duffing (vdPD) system and an energy harvesting (EH) system are studied to verify the feasibility and accuracy of the proposed approach. The measured data are simulated by the numerical results with the addition of the random noise in the following way:

$$\hat{\boldsymbol{R}} = \boldsymbol{R}_{\mathbf{cal}} + N_{\mathrm{level}} * \mathrm{Randn} * \mathrm{std}\left(\boldsymbol{R}_{\mathbf{cal}}\right) \tag{18}$$

where $\hat{\boldsymbol{R}}$ is the measured quantity contaminated by random noise, $\boldsymbol{R}_{\mathbf{cal}}$ is the corresponding numerical data, $std\left(\boldsymbol{R}_{\mathbf{cal}}\right)$ means the standard deviation of $\boldsymbol{R}_{\mathbf{cal}}$, N_{level} denotes the measurement noise level, and $Randn$ is the random noise with the standard normal distribution. Furthermore, the relative error is introduced in the following way to quantify the identification accuracy

$$\text{Relative error} = \frac{\boldsymbol{a_i}^{id} - \boldsymbol{a_i}^{ex}}{\boldsymbol{a_i}^{ex}} \times 100\% \tag{19}$$

where $\boldsymbol{a_i}^{id}$ is the identified value and $\boldsymbol{a_i}^{ex}$ corresponds to the exact value. The parameters of the enhanced response sensitivity approach in Table 1 are set as $tol = 10^{-10}$, $\sigma = \sqrt{2}$, $\theta_{cr} = 0.5$, $Nmax = 1000$, $Ntr = 20$.

4.1 van der Pol-Duffing system

The vdPD oscillator is one of the most extensively studied nonlinear systems with various engineering science applications. It is composed of a Duffing system with a cubic nonlinear restoring force term and a van der Pol system with a nonlinear damping term. Due to the vdPD

Table 1 The flow chart of the ERSA

Input: initial parameters $\boldsymbol{a}^{(0)}$, maximum iterations steps $Nmax$, maximum trust-region steps Ntr, error tolerance tol for convergence criterion.
Load the measurement data $\hat{\boldsymbol{R}}$, fix *trust-region* parameters $\vartheta \in [0.25, 0.75]$ and the amplification factor $\sigma > 1$
For $k = 1 : Nmax$
  Calculate the numerical response $\boldsymbol{R}\left(\boldsymbol{a}^{(k-1)}\right)$ of the nonlinear time-delay system based on the current parameters $\left(\boldsymbol{a}^{(k-1)}\right)$,
  Calculate the response sensitivity matrix $\boldsymbol{S}\left(\boldsymbol{a}^{(k-1)}\right)$ according to Eqs. (4) and (6), and calculate the residual $\delta \boldsymbol{R} = \hat{\boldsymbol{R}} - \boldsymbol{R}\left(\boldsymbol{a}^{(k-1)}\right)$,
  Use L-curve method to get the regularization parameters $\lambda_L(\boldsymbol{a}^{(k-1)})$,
  For $i = 1 : Ntr$
    Fix the regularization parameters $\lambda = \lambda_L(\boldsymbol{a}^{(k-1)})\sigma^{i-1}$,
    Calculate the update $\delta \boldsymbol{a}$ according to (13), **if** $(\boldsymbol{a}^{(k-1)} + \delta \boldsymbol{a}) \notin \mathbb{A}$,**continue**.
    Calculate the new response $\boldsymbol{R}\left(\boldsymbol{a}^{(k-1)} + \delta \boldsymbol{a}\right)$ and the new residual $\delta \boldsymbol{R}_{new} = \hat{\boldsymbol{R}} - \boldsymbol{R}\left(\boldsymbol{a}^{(k-1)} + \delta \boldsymbol{a}\right)$,
    Calculate the agreement indicator $\vartheta(\delta \boldsymbol{a}, \boldsymbol{a}^{(k-1)})$, **if** $\vartheta(\delta \boldsymbol{a}, \boldsymbol{a}^{(k-1)}) \geq \vartheta_{cr}$, **break**.
  End for
  Update the parameters $\boldsymbol{a}^{(k)} = \boldsymbol{a}^{(k-1)} + \delta \boldsymbol{a}$,
  If $\|\delta \boldsymbol{a}\| / \|\boldsymbol{a}^{(k)}\| \leq tol$, **break**.
End for

system containing complex nonlinear characteristics, it is a challenging task to estimate its parameters accurately and quickly, especially when the system contains time-delay feedback. Most of the existing work is based on meta-heuristics algorithms, and there is no time-delay in the system. For example, Quaranta et al. [33] have used particle swarm algorithm and differential evolution algorithm to identify the vdPD oscillators; Gao et al. [34] identified the uncertain parameters of the vdPD oscillators by a novel artificial bee colony algorithm with differential evolution operators. Goharoodi et al. [35] have identified the parameters of a real nonlinear Duffing oscillator by the alternating direction method. Different from the above work, this paper focuses on the parameter identification of vdPD system with time-delay.

A general form of vdPD system with the initial conditions can be described by the following equation:

$$\begin{cases} \ddot{x} + (\gamma x^2 - \alpha)\dot{x} + \omega_0^2 x + \beta x^3 = f\cos(\Omega t), \quad t > 0 \\ x(0) = x_0, \dot{x}(0) = \dot{x}_0 \end{cases} \tag{20}$$

where γ, α, ω_0 and β are the control parameters of the vdPD system, f and Ω are the parameters of the external excitation, $x(0)$ and $\dot{x}(0)$ are the initial displacement and velocity, respectively. The closed-loop vdPD system can be obtained by adding the time-delay feedback to the original equation, and there is [36]

$$\begin{cases} \ddot{x} + (\gamma x^2 - \alpha)\dot{x} + \omega_0^2 x + \beta x^3 \\ \quad = f\cos(\Omega t) + Ax(t - \tau_1) + Bx^3(t - \tau_2), \quad t > 0 \\ x(t) = x_0, \dot{x}(t) = \dot{x}_0, \quad t \leq 0 \end{cases} \tag{21}$$

where τ_1 and τ_2 are the delay parameters, and A, B are the corresponding feedback gains. The time-delay is named the negative feedback with $A, B < 0$ and positive feedback with $A, B > 0$. System (21) will reduce to system (20) with $\tau_1 = 0$ and $\tau_2 = 0$. For subsequent analysis, the system's parameters are fixed at $\gamma = 0.2, \alpha = 0.2, \omega_0 = 0.5, \beta = 0.3, A = 0.3, B = 0.2, \tau_1 = 0.5, \tau_2 = 0.8$, suppose the unknown parameters are $\boldsymbol{a} = (\gamma, \alpha, \omega_0, \beta, A, B, \tau_1, \tau_2)$, so there is $\boldsymbol{a} = (0.2, 0.2, 0.5, 0.3, 0.3, 0.2, 0.5, 0.8)$. The other parameters are fixed at $f = 1, \Omega = 0.3$. In order to verify the performance of the proposed approach, six cases named Case I-VI were selected to evaluate the effects of using different measurement data, different noise levels and different initial values. As shown in Table 2, the identification results of cases I-VI are presented in Table 3, where 'Iter #' represents the number of iterations.

Table 2 Parameter identification cases for time-delay vdPD system

Case	Initial parameters $\boldsymbol{a}^{(0)}$	Measurement data	Noise level e_v
I	[0.5,0.5,0.5,0.5,0.5,0.5,0.5,0.5]	$\ddot{x}$	0%
II	[0.5,0.5,0.5,0.5,0.5,0.5,0.5,0.5]	$\ddot{x}$	2%
III	[0.5,0.5,0.5,0.5,0.5,0.5,0.5,0.5]	$\ddot{x}$	5%
IV	[0.4,0.4,0.4,0.4,0.4,0.4,0.4,0.4]	$\ddot{x}$	5%
V	[0.5,0.5,0.5,0.5,0.5,0.5,0.5,0.5]	x	5%
VI	[0.5,0.5,0.5,0.5,0.5,0.5,0.5,0.5]	$x, \ddot{x}$	2%,5%

Table 3 Identification results and relative errors (% in brackets) of time-delay vdPD system

vdP system Exact values	γ 0.2	α 0.2	ω_0 0.5	β 0.3	A 0.3	B 0.2	τ_1 0.5	τ_2 0.8	Iter # /
Case I	0.2001	0.1978	0.4902	0.3001	0.2903	0.2001	0.5090	0.7998	31
	(0.037)	(−1.125)	(−1.952)	(0.021)	(−3.216)	(0.026)	(1.809)	(−0.026)	
Case II	0.1994	0.1987	0.4897	0.2996	0.2907	0.1998	0.5102	0.7995	50
	(−0.288)	(−0.665)	(−2.060)	(−0.139)	(−3.095)	(−0.101)	(2.304)	(−0.068)	
Case III	0.1983	0.2049	0.5102	0.2988	0.3096	0.1993	0.5063	0.7995	32
	(−0.855)	(2.432)	(2.039)	(−0.404)	(3.203)	(−0.334)	(1.260)	(−0.067)	
Case IV	0.1983	0.2048	0.5103	0.2988	0.3097	0.1993	0.5059	0.7995	9
	(−0.863)	(2.413)	(2.065)	(−0.399)	(3.249)	(−0.329)	(1.177)	(−0.066)	
Case V	0.1867	0.1811	0.5905	0.3083	0.3963	0.2086	0.3060	0.7918	23
	(−6.664)	(−9.443)	(18.107)	(2.753)	(32.099)	(4.323)	(−38.797)	(−1.026)	
Case VI	0.1997	0.2036	0.5002	0.2992	0.2999	0.1994	0.5201	0.7996	30
	(−0.143)	(1.780)	(0.035)	(−0.277)	(−0.041)	(−0.292)	(4.024)	(−0.047)	

The displacement and acceleration response are depicted in Fig. 1, which are obtained from numerical simulation during 30s with a sampling rate of 100Hz. Figure 1a displays the measured data without noise, and measured data with 5% noise level are shown in Fig. 1b. The response sensitivity with respect to $\boldsymbol{a}$ can be calculated according to Eqs. (4) and (5), and it is depicted in Fig. 2.

Firstly, as shown in Table 3, different noise levels are considered in cases I–III. Three cases have the same initial parameters, $\boldsymbol{a}^{(0)} = [0.5, 0.5, 0.5, 0.5, 0.5, 0.5, 0.5, 0.5]$. Noiseless response data were used for identification in Case I. In cases I–III, all parameters are well identified and parameter A has the highest relative error. Meanwhile, the maximum relative error of cases II and III is only 3.095% and 3.203%, respectively. The results show that the identification approach proposed in this paper seems insensitive to measurement noise. Even at the noise level of 5%, the relative error does not exceed 3.3% and identified results are quite gratifying.

Secondly, the effect of initial values on the identification is also investigated. The initial values of the unknown parameter are altered to $\boldsymbol{a}^{(0)} = [0.4, 0.4, 0.4, 0.4, 0.4, 0.4, 0.4, 0.4]$ in case IV, and the acceleration response with 5% random noise is still selected as the measurement data. As can be seen from Table 3, case IV has almost the same identification accuracy as case III and has less iteration steps. This indicates that the proposed approach is insensitive to the choice of the initial values.

Thirdly, different types of measurement data have been taken into account. Different from cases I–IV, the displacement response of the system is chosen as the measurement data in case V, which also contains 5% random noise, and the initial values are consistent with case III. It can be found from the results in Table 3 that although case V can also get the identification results, the accuracy is much lower than that of case III. More specifically, in case V τ_1 has a maximum relative error of 38.797%, but in case III the maximum relative error

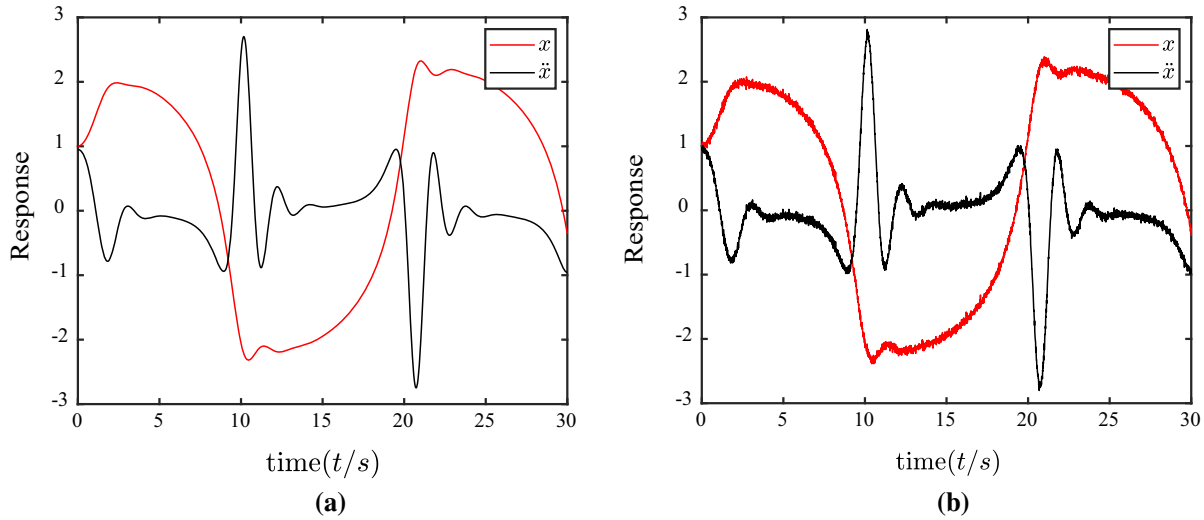

Fig. 1 The response of time-delay vdPD system: **a** without noise and **b** with noise

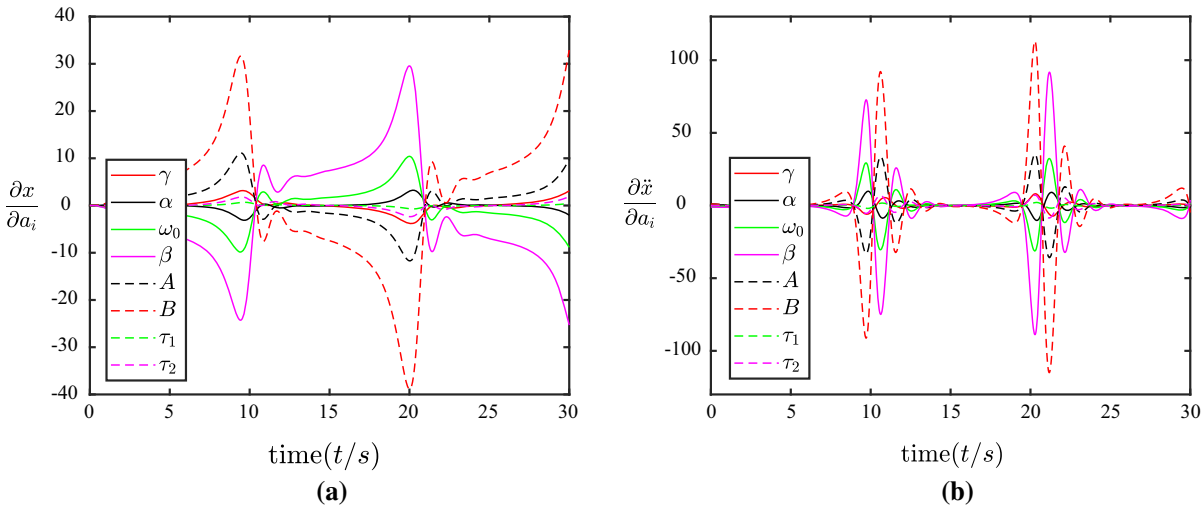

Fig. 2 The sensitivity response with respect to $\boldsymbol{a}$ of time-delay vdPD system: **a** displacement and **b** acceleration

is only 3.203%. This further shows that acceleration data has better anti-noise performance than displacement data. For case VI, the hybrid data are selected as the measurement data. Generally, more data can lead to a better result. The identification results of most parameters in case VI are better than those in case III, expect for τ_1. The maximum relative error is 4.024% in τ_1. Although the amount of the measurement data in case VI is more than that in case III, the number of iterations is of the same level. Such results prove that the proposed approach has good robustness for parameter identification of time-delay vdPD systems.

Finally, all iterations in cases I–VI are less than 50 steps. In order to observe the convergence procedure more intuitively, the evolution of identification parameters in cases I–VI are plotted in Fig. 3. It can be seen that all parameters converge very quickly, which further indicates that the proposed approach has good convergence. The final identification results of all cases are exhibited in Fig. 4.

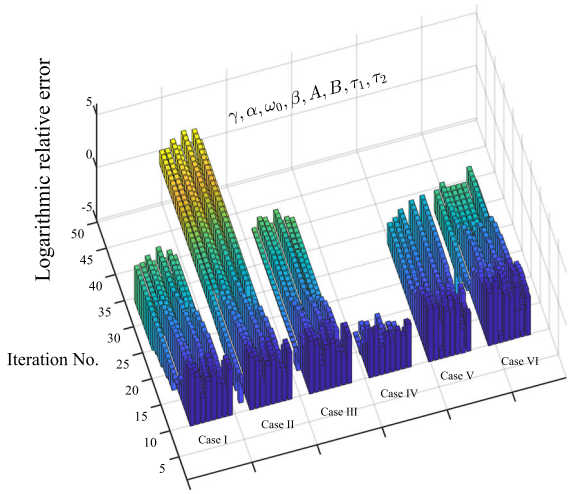

Fig. 3 Evolution of the parameters during iterations (cases I–VI) of time-delay vdPD system

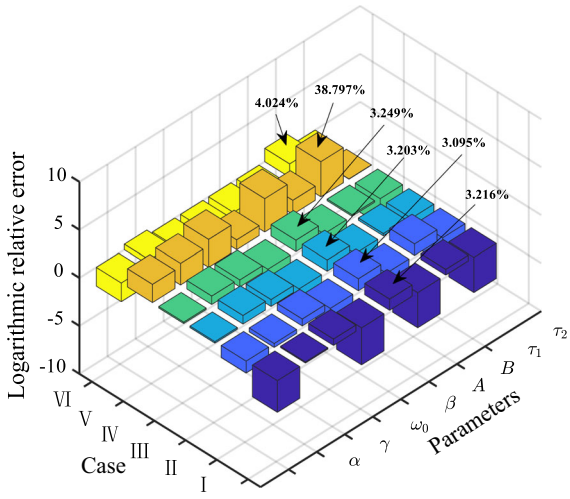

Fig. 4 The final identification results of cases I–VI of time-delay vdPD system

4.2 Energy harvesting system

Next, we consider an energy harvesting system with displacement delay. Vibration energy as the object of energy harvesting has broad development potential. Various forms of EH systems have been investigated to obtain energy from the vibration systems. Even in some applications, EH systems are also used in place of conventional shock absorbers [37]. The most common transducers are either types of piezoelectric or electromagnetic [38–40]. Moreover, recent studies have shown that quasi-periodic vibration can have a beneficial effect on the performance of time-delay EH system [41]. By the way, the evidence shows that the time-delay can enhance the performance of energy harvesting for Duffing-type nonlinear attachment [42].

As shown in Fig. 5, the EH device consists of an excited Duffing oscillator which is coupled with the circuit through piezoelectric ceramic layers. Such EH system can be described by a second-order and a first-order ordinary differential equation [43]

$$\begin{cases} \ddot{x} + \delta\dot{x} + \omega_0^2 x + \gamma x^3 - \chi v \\ \quad = \alpha x(t-\tau) + f\cos(\Omega t), \quad t > 0 \\ \dot{v} + \beta v + \kappa\dot{x} = 0 \\ x(t) = 1, v(t) = 0, \dot{x}(t) = 0, \dot{v}(t) = 0, \quad t \le 0 \end{cases} \tag{22}$$

Further, Eq. (22) can be rewritten as state-space form:

$$\begin{cases} \begin{pmatrix} \dot{x} \\ \ddot{x} \\ \dot{v} \end{pmatrix} = \begin{pmatrix} 0 & 1 & 0 \\ -\omega_0^2 & -\delta & \chi \\ 0 & -\kappa & -\beta \end{pmatrix} \begin{pmatrix} x \\ \dot{x} \\ v \end{pmatrix} \\ \quad + \begin{pmatrix} 0 \\ -\gamma x^3 + \alpha x(t-\tau) + f\cos(\Omega t) \\ 0 \end{pmatrix}, \quad t > 0 \\ x(t) = 1, v(t) = 0, \dot{x}(t) = 0, \dot{v}(t) = 0, \quad t \le 0 \end{cases} \tag{23}$$

where x is the displacement of the mass m, the dot over the variables represents the derivative with respect to the time t, δ is the damping ratio, ω_0 is the linear frequency, γ is the nonlinear stiffness, χ is the piezoelectric coupling coefficient, v is the voltage at the resistance, β is the piezoelectric coefficient, κ is the damping ratio of piezoelectric ceramic layers, τ and α are the time-delay parameter and the corresponding feedback gain, respectively. f and Ω are the amplitude and frequency of the external excitation, respectively. The

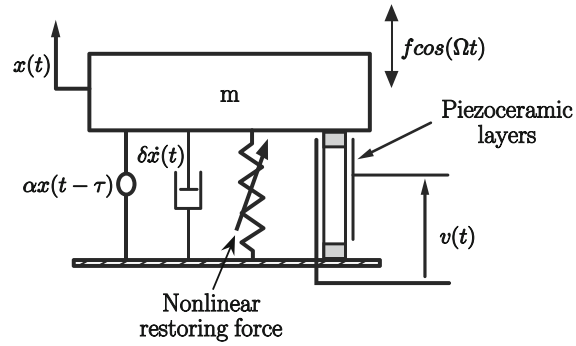

Fig. 5 Sketch of the EH system

above parameters are fixed at $\delta = 0.1, \omega_0 = 1, \gamma = 0.25, \chi = 0.05, \alpha = 0.2, f = 0.2, \beta = 0.05, \kappa = 0.5, \tau = 4.8, \Omega = 1.25$. Further, suppose the unknown parameters are $\boldsymbol{a} = (\delta, \omega_0, \gamma, \chi, \alpha, f, \beta, \kappa, \tau)$, so $\boldsymbol{a} = (0.1, 1, 0.25, 0.05, 0.2, 0.2, 0.05, 0.5, 4.8)$.

The numerical response is also obtained by the 'dde23' function in MATLAB, and the measured data are simulated according to Eq. (18) during the time $T = [0s, 30s]$ with a sampling rate of 100 Hz. Six cases named as Case I*–VI* listed in Table 4, are taken into account to evaluate the feasibility of the proposed approach for time-delay EH system. The identification results of all caves also are summarized in Table 5. The displacement of x and v without noise and with 5% random noise is depicted in Fig. 6. The sensitivity response with respect to the unknown parameters also can be calculated by Eq. (4) in each iteration. As shown in Fig. 7, it is the displacement sensitivity response of the EH system with $\boldsymbol{a} = (0.1, 1, 0.25, 0.05, 0.2, 0.2, 0.05, 0.5, 4.8)$.

Firstly, different types of measurement data without noise are considered in cases I*–II*, as depicted in Fig. 6a. The measurement data of case I* only contain the voltage at the resistance v, while case II* contains both x. It can be seen from the identification results in Table 5 that both cases have obtained accurate parameters. Case I* shows that for time-delay EH system, even if only voltage data, the unknown parameters can be accurately identified, which is obviously of great significance for practical engineering. Because the voltage data can be obtained only through the voltage measuring device inside the circuit, but the displacement data of mass m usually need additional laser rangefinder. However, since the amount of measurement data contained in case II* is twice as much as that of the case I*, case II* has fewer iteration steps.

The measurement data x with 3% noise, v with 5% noise are used for identification in case III*. Cases I*–III* keep the same initial values $\boldsymbol{a}^{(0)} = [0.4, 0.4, 0.4, 0.4, 0.4, 0.4, 0.4, 0.4, 4]$, and then iden-

Table 4 Parameter identification cases for EH system

Case	Initial parameters $\boldsymbol{a}^{(0)}$	Measurement data	Noise level e_v	Weight matrix
I*	[0.4,0.4,0.4,0.4,0.4,0.4,0.4,0.4,4]	v	0%	$\boldsymbol{I}$
II*	[0.4,0.4,0.4,0.4,0.4,0.4,0.4,0.4,4]	x, v	0%, 0%	$\boldsymbol{I}$
III*	[0.4,0.4,0.4,0.4,0.4,0.4,0.4,0.4,4]	x, v	3%, 5%	$\boldsymbol{I}$
IV*	[0.5,0.5,0.5,0.5,0.5,0.5,0.5,0.5,5]	x, v	3%, 5%	$\boldsymbol{I}$
V*	[0.5,0.5,0.5,0.5,0.5,0.5,0.5,0.5,5]	x, v	3%, 5%	$\boldsymbol{W}^{\mathbf{opt}}$
VI*	[0.5,0.5,0.5,0.5,0.5,0.5,0.5,0.5,5]	x, v	10%, 10%	$\boldsymbol{W}^{\mathbf{opt}}$

(I) means identify matrix and (W^{opt}) means the optimal weight matrix

Table 5 Identified results and relative errors (% in brackets) of EH system

EH system Exact values	δ 0.1	ω_0 1	γ 0.25	χ 0.05	α 0.2	f 0.2	β 0.05	κ 0.5	τ 4.8	Iter # /
Case I*	0.1000	0.9999	0.2501	0.0504	0.1999	0.2000	0.0500	0.5001	4.7999	93
	(0.001)	(−0.010)	(0.029)	(0.765)	(−0.011)	(0.002)	(0.021)	(0.017)	(−0.001)	
Case II*	0.1003	1.0002	0.2499	0.0495	0.2002	0.2002	0.0500	0.5000	4.7989	57
	(0.279)	(0.017)	(−0.022)	(−1.070)	(0.087)	(0.094)	(0.008)	(0.001)	(−0.022)	
Case III*	0.1006	1.0005	0.2510	0.0464	0.2016	0.1996	0.0502	0.5001	4.7982	50
	(0.629)	(0.049)	(0.392)	(−7.119)	(0.814)	(−0.197)	(0.302)	(0.024)	(−0.037)	
Case IV*	0.1006	1.0005	0.2510	0.0465	0.2016	0.1996	0.0502	0.5001	4.7983	64
	(0.613)	(0.048)	(0.394)	(−7.053)	(0.808)	(−0.203)	(0.302)	(0.024)	(−0. 036)	
Case V*	0.1006	1.0004	0.2507	0.0470	0.2012	0.1998	0.0501	0.5001	4.7982	101
	(0.607)	(0.046)	(0.278)	(−5.968)	(0.621)	(−0.091)	(0.288)	(0.023)	(−0.038)	
Case VI*	0.1010	1.0008	0.2508	0.0453	0.2014	0.2000	0.0503	0.5002	4.7972	66
	(0.954)	(0.081)	(0.317)	(−9.427)	(0.688)	(0.002)	(0.533)	(0.041)	(−0.059)	

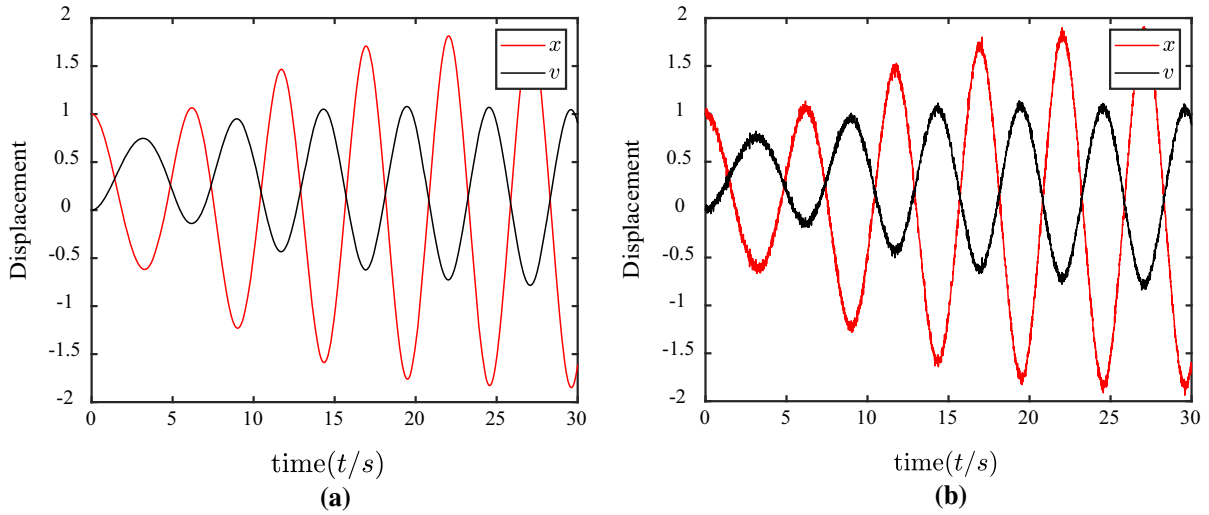

Fig. 6 The displacements of EH system: **a** without noise and **b** with random noise

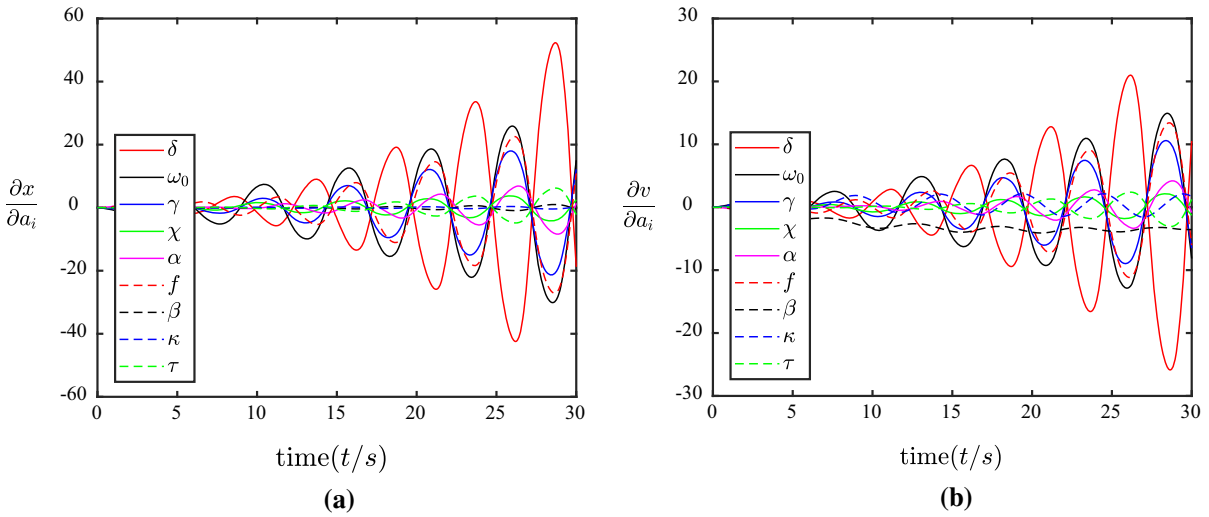

Fig. 7 The displacement sensitivity response with respect to $\boldsymbol{a}$ of EH system

tification results were well obtained and the maximum relative errors are 0.765%, 1.070% and 7.119% in χ, respectively. This indicates that although the measurement noise will reduce the accuracy of the identified results, the proposed approach can obtain the usable results from the noisy data.

Similar to previous vdPD system, we will also discuss the influence of different initial values on identification. The initial values of the parameters are changed into $\boldsymbol{a}^{(0)} = [0.5, 0.5, 0.5, 0.5, 0.5, 0.5, 0.5, 0.5, 5]$ in case IV*. It is seen that the maximum relative error arising at χ is 7.053%, so for case IV*, the maximum relative error and the number of iteration steps are at the same level as case III*. These two initial parameters can lead to convergent and satisfactory results. This shows that the ERSA has good convergence even for relatively complex systems.

Next, we will focus on the influence of the weight matrix on the parameter identification of the time-delay EH system. As described in Sect. 3, a good weight matrix can lead to better identification accuracy. In case V*, the initial parameter and noise level are set as the same with those in case IV*. And the optimal weight matrix $\boldsymbol{W}^{\mathbf{opt}}$ is chosen as the reciprocal of the covari-

ance of measurement data error. From Table 5 we can find that the maximum relative error χ is reduced form 7.053% to 5.968%. This is because the optimal weight matrix selected in this paper can make the measurement data with higher noise level occupy a smaller weight in the identification process. In case VI*, when the measurement noise level reaches 10% in x and v, the maximum relative error arrives at χ is 9.427%. Nevertheless, the absolute error of χ is merely 0.0047. The robustness of the proposed method has been verified by this case. Finally, the evolution of the parameters during the iterations of the time-delay EH system is plotted in Fig. 8. The identification results begin to converge after about 40 steps. Indeed, the identification results show that the approach can converge fast and achieve high accuracy. Figure 9 presents the relative errors of the identification results for these six cases.

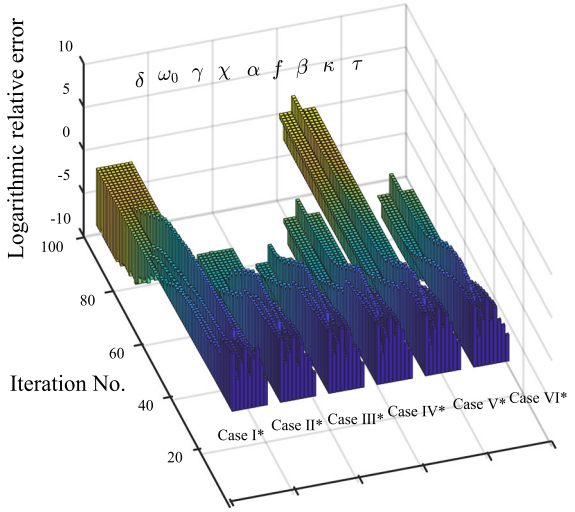

Fig. 8 Evolution of the parameters during iterations (cases I*–VI*) of EH system

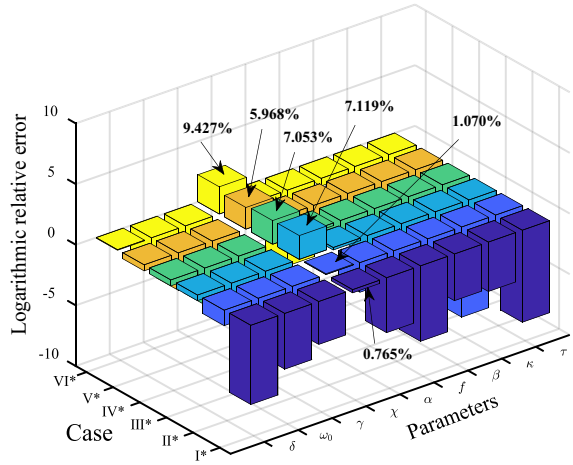

Fig. 9 The final identification results of cases I*–VI* of EH system

5 Experimental verification

In this section, the Mackey-Glass time-delay system was investigated to verify the effectiveness of the proposed approach by the numerical simulation and circuit experiments. In 1977, the Mackey-Glass system was first proposed by Mackey and Glass to illustrate the dynamics diseases in the physiological system (respiratory and hematopoietic diseases) [44]. For some physiological diseases, the physiological variables are usually closely related to medicine intake. However, due to the lag of drug absorption in the physiological system, the physiological system with relation to the environmental changes is a typical nonlinear time-delay system [45]. Over the years, the Mackey-Glass model has been investigated frequently, and it has widely arisen in hematology, cardiology, neurology and psychiatry [46]. The Mackey-Glass system can be described by the following nonlinear time-delay differential equation:

$$\begin{cases} \dot{x} = \dfrac{\beta x(t-\tau)}{1+x^n(t-\tau)} - \gamma x, \quad \gamma, \beta, n, t > 0 \\ x(t) = 0.5, \quad t \le 0 \end{cases} \tag{24}$$

where β, γ, n and τ are the control parameters. Assumed that these parameters are all unknown, i.e., $\boldsymbol{a} = (\beta, \gamma, n, \tau)$, and the parameters are fixed at $\beta = 2$, $\gamma = 1$, $n = 7$, $\tau = 2$ in the simulations, so $\boldsymbol{a} = (2, 1, 7, 2)$. The numerical response is exhibited in Fig. 10 with the sampling duration 150s, and the sampling frequency 100 Hz. The time histories without noise were shown on the left, and the right was the phase diagram.

Besides, the Mackey-Glass model can also be implemented by an electronic circuit. The main parts of the electronic implementation are the following: two passive elements, Resistance (**R**) and Capacitance (**C**); the delay block, which produces a time offset between the input and the output; and the nonlinear function **F**(**v**). A schematic view of the electronic circuit is shown in Fig.11, and a detailed description can be found in [47,48]. The control parameters $\boldsymbol{a}$ of the experimental circuit are set as $\beta = 3.73$, $\gamma = 1$, $n = 4$. As shown in Fig. 12 are the steady-state response curves of system

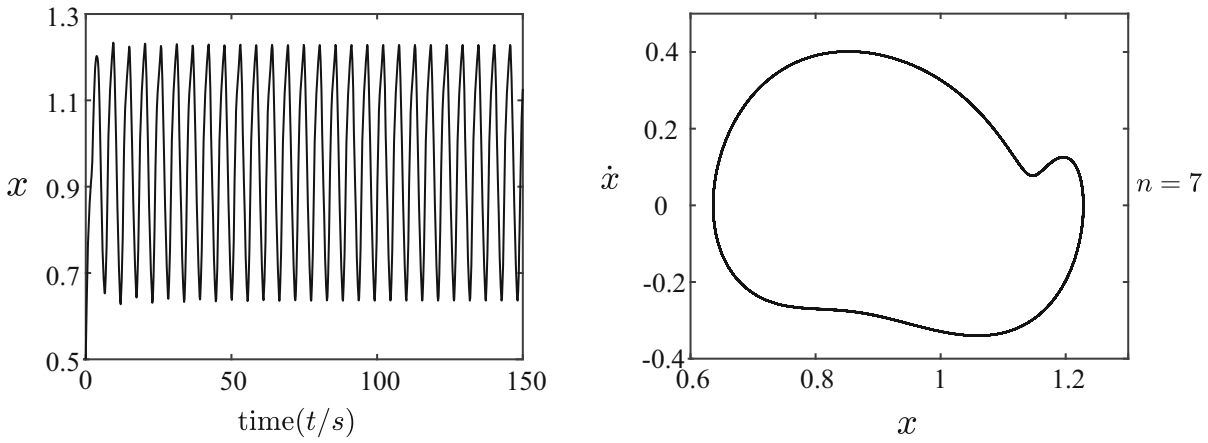

Fig. 10 The response of the nonlinear Mackey-Glass time-delay system

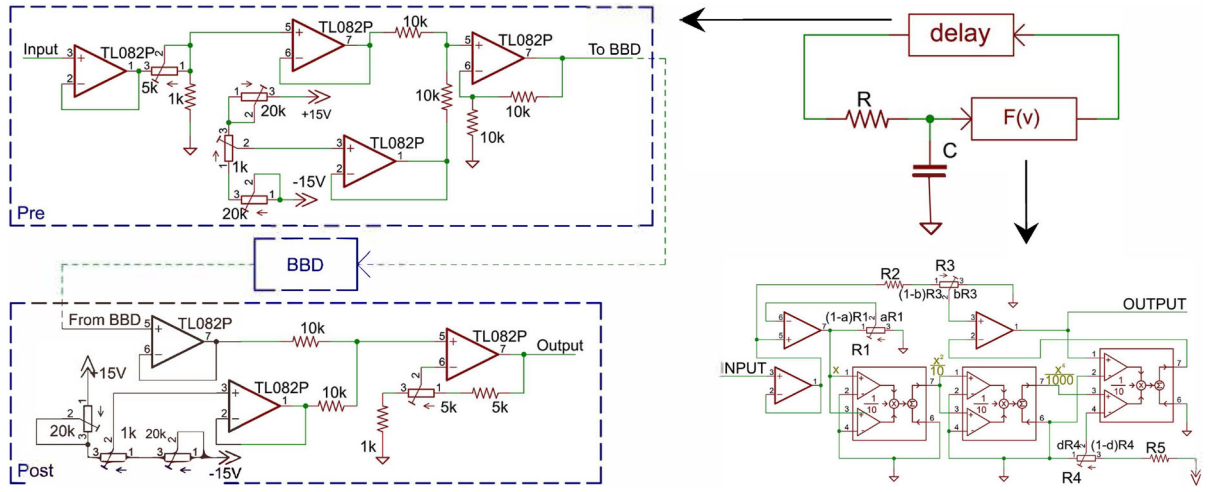

Fig. 11 Circuit schematic of the nonlinear Mackey-Glass time-delay system [47]

(24) with different delay τ. It should be noted that in the real experiment, it is difficult to measure the initial transient response data, and usually only the steady-state response of the system can be measured. Therefore, the measured steady-state response data will be directly used in this experimental example. It can be seen from the figure that whether $\tau = 5$ (Fig. 12a) or $\tau = 7$ (Fig. 12b), the experimental results of electronic circuits and the numerical results show a great deal of concordance. It can be further found that the period of the system increases with the increase in the time-delay τ. However, the analytical curves do not completely coincide with the experimental curves at the peak. This may be due to the measurement error of the experiment.

Different types of measured data and initial parameters of simulated and experimental cases are listed in Table 6. The expressions of the response sensitivity $\frac{\partial \dot{x}}{\partial a_i}$ with respect to the parameters are obtained as below:

$$\begin{cases} \dfrac{\partial \dot{x}}{\partial \beta} = \dfrac{\beta\left(1+(1-n)x_\tau^n\right)}{(1+x_\tau^n)^2}\dfrac{\partial x_\tau}{\partial \beta} - \gamma\dfrac{\partial x}{\partial \beta} + \dfrac{x_\tau}{1+x_\tau^n} \\ \dfrac{\partial \dot{x}}{\partial \gamma} = \dfrac{\beta\left(1+(1-n)x_\tau^n\right)}{(1+x_\tau^n)^2}\dfrac{\partial x_\tau}{\partial \gamma} - \gamma\dfrac{\partial x}{\partial \gamma} - x \\ \dfrac{\partial \dot{x}}{\partial n} = \dfrac{\beta\left(1+(1-n-x_\tau log_{10} x_\tau)x_\tau^n\right)}{(1+x_\tau^n)^2}\dfrac{\partial x_\tau}{\partial n} - \gamma\dfrac{\partial x}{\partial n} \\ \dfrac{\partial \dot{x}}{\partial \tau} = \dfrac{\beta\left(1+(1-n)x_\tau^n\right)}{(1+x_\tau^n)^2}\left(\dfrac{\partial x_\tau}{\partial \tau} - \dot{x}_\tau\right) - \gamma\dfrac{\partial x}{\partial \tau} \end{cases} \tag{25}$$

where $x(t-\tau)$ is abbreviated as x_τ. The response sensitivity in time-domain can be calculated according to

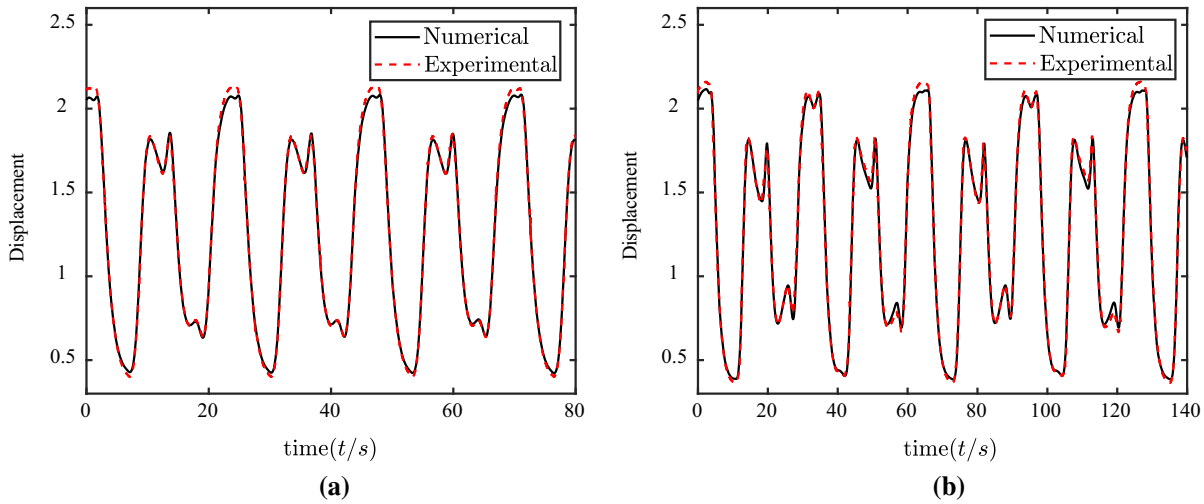

Fig. 12 The numerical (black lines) and experimental (red dotted lines) displacement response. **a** $\tau = 5$, **b** $\tau = 7$ [47]

Table 6 Parameter identification cases of the nonlinear Mackey-Glass time-delay system

(I) means identify matrix and (W^{opt}) means the optimal weight matrix

Case	Exact parameters $\boldsymbol{a}$	Initial parameters $\boldsymbol{a}^{(0)}$	Measurement data	Noise level e_v	Weight matrix
I**	[2,1,7,2]	[3,3,3,3]	$x, \dot{x}$	0%, 0%	$\boldsymbol{I}$
II**	[2,1,7,2]	[3,3,3,3]	$x, \dot{x}$	3%, 5%	$\boldsymbol{W}^{\text{opt}}$
III**	[3.73,1,4,5]	[3;1.5;4.5;4.5]	x	experimental	$\boldsymbol{I}$
IV**	[3.73,1,4,7]	[3;1.5;4.5;7.5]	x	experimental	$\boldsymbol{I}$

Table 7 Identified parameters and relative errors (% in brackets) of the nonlinear Mackey-Glass time-delay system

Mackey-Glass system	β	γ	n	τ	Iter #
Case I**	1.9998	0.9999	7.0005	1.9999	41
	(−0.009)	(−0.009)	(0.007)	(−0.002)	
Case II**	2.0006	1.0003	7.0027	2.0002	41
	(0.029)	(0.027)	(0.039)	(0.011)	
Case III**	3.6081	0.9513	4.0348	4.9641	10
	(−3.268)	(−4.867)	(0.870)	(−0.717)	
Case IV**	3.6087	0.9583	4.0328	6.9710	37
	(−3.253)	(−4.172)	(0.819)	(−0.414)	

Eq. (24) and (25). The identified results and the relative errors of this system were obtained by ERSA, and they are shown in Table 7. Moreover, Fig. 13 shows the identification process of all cases, and the final identification results are summarily exhibited in Fig. 14.

Firstly, case I** and case II** were the numerical cases with the same initial parameters $\boldsymbol{a}^{(0)} = [3, 3, 3, 3]$. Two cases are intended to consider the effect of the measurement noise. The case I** has the accurate identified results and its relative errors almost equal to 0. The measured data in case II** are x with 3% noise, $\dot{x}$ with 5% noise, and the optimal weight matrix $\boldsymbol{W}^{\text{opt}}$ are taken for this case because $\boldsymbol{W}^{\text{opt}}$ gives superior identification results in the previous example. Obviously, the unknown parameters are also precisely identified from the noisy time-domain data. In case I**, parameters β and n have a lager relative error of 0.009%, and the maximum relative error of case

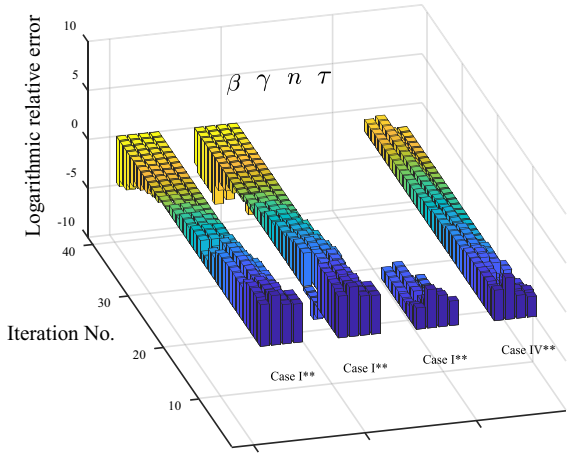

Fig. 13 Evolution of the parameters during iterations (cases I**–IV**) of the nonlinear Mackey-Glass time-delay system

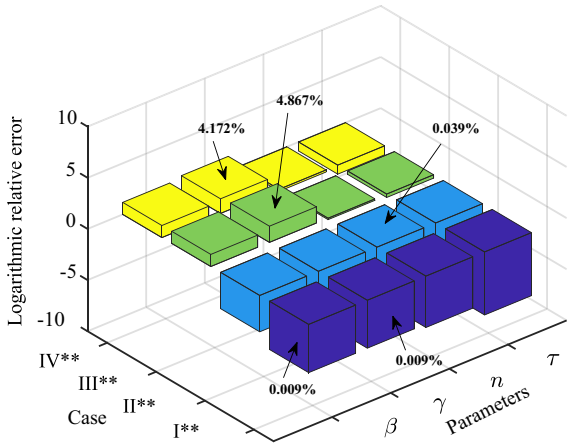

Fig. 14 The final identification results of cases I**–IV** of the nonlinear Mackey-Glass time-delay system

II** is 0.039% appearing in β. The iteration converges quicker, and the relative error is also slight. All identifications are all convergent in around 40 iterations which indicates that the proposed approach is rather quickly efficient.

There are different control parameters in the real experimental circuit. Only response data x were measured to test whether it is compatible with parameter identification. The real experimental parameters in case III** are $\boldsymbol{a} = [3.73, 1, 4, 5]$, while $\tau = 7$ in case IV**. In case III*, the identification procedure of the parameters is rapidly identified within 10 iterations, and the highest relative error is 4.867% in γ, which is much higher than the numerical cases. The difference between the peak shown in Fig. 12 may cause this situation. The highest relative error 4.172% in the identified results of case IV** appears in γ, and the identification process needs 37 iterations. Finally, we can find that the ERSA can still identify the system parameters precisely even from the real noisy time-domain data, especially the delay parameter τ and its coefficient β. The experimental cases proved that the proposed approach is competent for nonlinear time-delay systems in engineering.

6 Conclusions

In this paper, an enhanced response sensitivity approach (ERSA) has been established to identify the parameters of various nonlinear time-delay systems from the time-domain data. Such a parameter identification problem is modeled as a typical nonlinear least-square optimization problem and solved iteratively by a gradient-based method. For the further sensitivity analysis, we take a general nonlinear time-delay system as an example to derive the sensitivity equations of delay terms and other parameters, and the ill-posed problems in the iterative process also tackled by the Tikhonov regularization. Furthermore, the *trust-region constraint* is proposed to make the ERSA suitable for strongly nonlinear systems. Two numerical examples and an experimental test are studied, and results conclude as

- The proposed approach can identify the parameters of nonlinear time-delay system from the time-domain response data accurately and rapidly.
- The proposed approach has a good anti-noise performance, even if the measured data contain 10% random noise, and it can also obtain good identification results.
- The proposed approach is insensitive to the choice of initial values.
- Numerical examples show that the hybrid data can lead to a better identification, and the influence of measurement noise can be reduced by the optimal weight matrix.
- The experimental tests show that the proposed approach can obtain satisfactory identification results even with steady-state measurement data with measurement errors, especially for the delay terms and its coefficients.

Thus, it is believed that the present ERSA will be a reliable and efficient tool for parameter identification of general nonlinear time-delay systems.

Acknowledgements The present investigation was performed under the support of National Natural Science Foundation of China (No. 11702336, No. 11972380), Guangdong Province Natural Science Foundation (No. 2017A030313007) and the Fundamental Research Funds of the Central Universities (No. 17lgpy54).

Compliance with ethical standards

Conflicts of interest The authors declare that they have no conflict of interest.

References

1. Yaghoobi, S., Moghaddam, B.P., Ivaz, K.: An efficient cubic spline approximation for variable-order fractional differential equations with time delay. Nonlinear Dyn. **87**(2), 815–826 (2017)
2. Masamura, S., Iwamoto, T., Sugitani, Y., Konishi, K., Hara, N.: Experimental investigation of amplitude death in delay-coupled double-scroll circuits with randomly time-varying network topology. Nonlinear Dyn. **1–14**, 3155–3168 (2020)
3. Tlidi, M., Panajotov, K.: Two-dimensional dissipative rogue waves due to time-delayed feedback in cavity nonlinear optics. Chaos Interdiscip. J. Nonlinear Sci. **27**(1), 013119 (2017)
4. Cui, Y.J., Xiao, S.P., Xiao, H.Q.: A survey on stability of time-delay and networked systems-from nanometer, biology, economy to electricity. Nanosci. Nanotechnol. Lett. **11**(9), 1185–1199 (2019)
5. Tsai, Y.Y., Chen, K.J., Yang, Y.H., Lin, Y.H.: Use of traditional Chinese medicine may delay the need for insulin treatment in patients with type 2 diabetes: a population-based cohort study. J. Alternat. Complem. Med. **26**(7), 628–635 (2020)
6. Lakshmanan, M., Senthilkumar, D.V.: Dynamics of nonlinear time-delay systems. Springer, New York (2011)
7. Richard, J.P.: Time-delay systems: an overview of some recent advances and open problems. Automatica **39**(10), 1667–1694 (2003)
8. Lin, Q., Loxton, R., Xu, C., Teo, K.L.: Parameter estimation for nonlinear time-delay systems with noisy output measurements. Automatica **60**, 48–56 (2015)
9. Chen, Y., Cheng, J., Jiang, Y., Liu, K.J.: A time delay dynamical model for outbreak of 2019-nCoV and the parameter identification. J. Inv. Ill Posed Prob. **28**(2), 243–250 (2020)
10. Wang, H.Q., Liu, P.X., Shi, P.: Observer-based fuzzy adaptive output-feedback control of stochastic nonlinear multiple time-delay systems. IEEE Trans. Cybern. **47**(9), 2568–2578 (2017)
11. Liu, G., Wang, L., Liu, J.K., Chen, Y.M., Lu, Z.R.: Identification of an airfoil-store system with cubic nonlinearity via enhanced response sensitivity approach. AIAA J. **56**(11), 4977–4987 (2018)
12. Yang, Z.Y., Seested, G.T.: Time-delay system identification using genetic algorithm-part one: precise fopdt model estimation. IFAC Proc. Vol. **46**(20), 561–567 (2013)
13. Gao, F., Fei, F.X., Xu, Q., Deng, Y.F., Qi, Y.B., Balasingham, I.: A novel artificial bee colony algorithm with space contraction for unknown parameters identification and time-delays of chaotic systems. Appl. Math. Comput. **219**(2), 552–568 (2012)
14. Tang, Y.G., Guan, X.P.: Parameter estimation for time-delay chaotic system by particle swarm optimization. Chaos Solitons Fract. **40**(3), 1391–1398 (2009)
15. Tang, Y.G., Cui, M.Y., Li, L.X., Peng, H.P., Guan, X.P.: Time-delay system identification using genetic algorithm-part one: precise fopdt model estimation. IFAC Proc. Vol. **41**(4), 2097–2102 (2009)
16. Ding, F., Liu, X.P., Liu, G.J.: Identification methods for Hammerstein nonlinear systems. Dig. Signal Process. **21**(2), 215–238 (2011)
17. Lund, A., Dyke, S.J., Song, W., Bilionis, I.: Global sensitivity analysis for the design of nonlinear identification experiments. Nonlinear Dyn. **98**(1), 375–394 (2019)
18. Lu, Z.R., Law, S.S.: Features of dynamic response sensitivity and its application in damage detection. J. Sound Vib. **303**(1–2), 305–329 (2007)
19. Lu, Z.R., Wang, L.: An enhanced response sensitivity approach for structural damage identification: convergence and performance. Int. J. Numer. Methods Eng. **111**(13), 1231–1251 (2017)
20. Wang, L., Liu, J.K., Lu, Z.R.: Incremental response sensitivity approach for parameter identification of chaotic and hyperchaotic systems. Nonlinear Dyn. **89**(1), 153–167 (2017)
21. Lu, Z.R., Liu, G., Liu, J.K., Chen, Y.M., Wang, L.: Parameter identification of nonlinear fractional-order systems by enhanced response sensitivity approach. Nonlinear Dyn. **95**(2), 1495–1512 (2018)
22. Liu, G., Wang, L., Liu, J.K., Chen, Y.M., Lu, Z.R.: Parameter identification of fractional order system using enhanced response sensitivity approach. Commun. Nonlinear Sci. Numer. Simul. **67**, 492–505 (2019)
23. Björklund, S., Ljung, L.: An improved phase method for time-delay estimation. Automatica **45**(10), 2467–2470 (2009)
24. Zhang, X.X., Xu, J.: Time-Delay Identification for Linear Systems: A Practical Method Using the Frequency Response Function. Springer, New York (2017)
25. Liu, G., Yu, M.L., Wang, L., Yin, Z.Y., Liu, J.K., Lu, Z.R.: Rapid parameter identification of linear time-delay system from noisy frequency domain data. Appl. Math. Model. **83**, 736–753 (2020)
26. Zhang, X.X., Xu, J.: Identification of time delay in nonlinear systems with delayed feedback control. J. Frankl. Instit. **352**(8), 2987–2998 (2015)
27. Zhang, X., Xu, J., Feng, Z.: Nonlinear equivalent model and its identification for a delayed absorber with magnetic action using distorted measurement. Nonlinear Dyn. **88**(2), 937–954 (2017)
28. Zhang, X., Ji, J., Xu, J.: Parameter identification of time-delayed nonlinear systems: an integrated method with adap-

tive noise correction. J. Frankl. Instit. **356**(11), 5858–5880 (2019)
29. Bellen, A., Zennaro, M.: Numerical methods for delay differential equations. Oxford University Press, Oxford (2013)
30. Lu, Z.R., Zhou, J.X., Wang, L.: On choice and effect of weight matrix for response sensitivity-based damage identification with measurement and model errors. Mech. Syst. Signal Process. **114**, 1–24 (2019)
31. Liu, G., Wang, L., Liu, J.K., Lu, Z.R.: Parameter identification of nonlinear aeroelastic system with time-delayed feedback control. AIAA J. **58**(1), 415–425 (2020)
32. Liu, G., Wang, L., Luo, W.L., Liu, J.K., Lu, Z.R.: Parameter identification of fractional order system using enhanced response sensitivity approach. Commun. Nonlinear Sci. Numer. Simul. **67**, 492–550 (2019)
33. Quaranta, G., Monti, G., Marano, G.C.: Parameters identification of Van der Pol-Duffing oscillators via particle swarm optimization and differential evolution. Mech. Syst. Signal Process. **24**(7), 2076–2095 (2010)
34. Gao, F., Lee, X.J., Fei, F.X., Tong, H.Q., Qi, Y.B., Deng, Y.F., Balasingham, I., Zhao, H.L.: Parameter identification for Van Der Pol-Duffing oscillator by a novel artificial bee colony algorithm with differential evolution operators. Appl. Math. Comput. **222**, 132–144 (2013)
35. Goharoodi, S.K., Dekemele, K., Dupre, L., Loccufier, M., Crevecoeur, G.: Sparse identification of nonlinear duffing oscillator from measurement data. IFAC-PapersOnLine **51**(33), 162–167 (2018)
36. Xu, J., Chung, K.W.: Effects of time delayed position feedback on a van der Pol-Duffing oscillator. Phys. D Nonlinear Phenom. **180**(1–2), 17–39 (2003)
37. Li, Z.J., Zuo, L., Luhrs, G., Lin, L.J., Qin, Y.X.: Electromagnetic energy-harvesting shock absorbers: design, modeling, and road tests. IEEE Trans. Vehic. Technol. **62**(3), 1065–1074 (2012)
38. Khaligh, A., Zeng, P., Zheng, C.: Kinetic energy harvesting using piezoelectric and electromagnetic technologies-state of the art. IEEE Trans. Vehic. Technol. **57**(3), 850–860 (2009)
39. Karami, M.A., Inman, D.J.: Equivalent damping and frequency change for linear and nonlinear hybrid vibrational energy harvesting systems. J. Sound Vib. **330**(23), 5583–5597 (2011)
40. Iliuk, I., Balthazar, J.M., Tusset, A.M., Piqueira, J.R., de Pontes, B.R., Felix, J.L., Bueno, A.M.: Application of passive control to energy harvester efficiency using a nonideal portal frame structural support system. J. Intell. Mater. Syst. Struct. **25**(4), 417–429 (2014)
41. Belhaq, M., Hamdi, M.: Energy harvesting from quasi-periodic vibrations. Nonlinear Dyn. **86**(4), 2193–2205 (2016)
42. Kammer, A.S., Olgac, N.: Delayed-feedback vibration absorbers to enhance energy harvesting. J. Sound Vib. **363**, 54–67 (2016)
43. Ghouli, Z., Hamdi, M., Lakrad, F., Belhaq, M.: Quasiperiodic energy harvesting in a forced and delayed Duffing harvester device. J. Sound Vib. **407**, 271–285 (2017)
44. Mackey, M., Glass, L.: Oscillation and chaos in physiological control systems. Science **197**(4300), 287–289 (1977)
45. Glass, L., Mackey, M.: Mackey-Glass equation. Scholarpedia **5**(3), 6908 (2010)
46. Bélair, J.: Dynamical Disease: Mathematical Analysis of Human Illness. American Institute of Physics Press, New York (1995)
47. Amil, P., Cabeza, C., Marti, A.C.: Exact discrete-time implementation of the Mackey-Glass delayed model. IEEE Trans. Circ. Syst. II Exp. Briefs **62**(7), 681–685 (2015)
48. Amil, P., Cabeza, C., Marti, A.C.: Electronic Implementation of the Mackey-Glass Delayed Model. arXiv. (2014)